

Turbulent Transition Prediction Using Large-Eddy Simulation with the Stability Theory

M. Kim*, J. Lim*, S. Kim*, S. Jee*, J. Park** and D. Park**

Corresponding author: sjee@gist.ac.kr

* Gwangju Institute of Science and Technology, KOREA

** Pusan National University, KOREA.

Abstract: Turbulent transition critically impacts on aerodynamic performance of aircraft, e.g., aerodynamic drag and fuel efficiency. Therefore, it is required for engineers to be able to predict turbulent transition. Large-eddy simulation (LES) coupled with the stability theory is proposed in this study. For cost-effective computations, the stability analysis is performed in the pre-transition region, and LES is used to describe the turbulent boundary layer with high accuracy. To demonstrate the feasibility of LES coupled with the stability theory, a canonical case of the flat-plate boundary layer is simulated. Two dominant instabilities, 2D Tollmien-Schlichting and 3D oblique waves, are determined and fed into the LES inlet. Staggered lambda structures, one of characteristics of natural transition, are well reproduced in the transition region. In addition, hairpin vortices inside turbulent boundary layer are clearly captured. Current simulation results are compared to experiment and direct-numerical simulation data including the skin friction and details of major instability modes.

Keywords: Boundary Layer, Large-Eddy Simulation, Turbulence Transition, Stability Analysis.

1 Introduction

Laminar-to-turbulent transition is a critical phenomenon, impacting aerodynamic performances of aircraft. Significant region of laminar flow on aircraft surface could reduce the aerodynamic drag, which helps to achieve in high fuel efficiency. In consequence, it is required for engineers to be able to predict the turbulent transition in a wall-boundary layer.

Natural transition is of interest to the current numerical study because this transition process is related to moving vehicles in air and water at nominal cruising conditions. In the first stage of the natural transition, disturbance waves come into the boundary layer and then slowly grow in the linear-growth region. When nonlinear interactions of multiple disturbances of large enough amplitudes occur, vortical structures including so-called Λ -structure emerge in the turbulent transition region. A specific type of the natural transitions can be determined through vortical structures. Staggered Λ -structures are observed in H-type transition, whereas aligned Λ -structures are observed in K-type transition. The H-type transition is numerically studied in this study.

The linear stability theory (LST) has been used for the transition prediction over decades. LST, however, is limited to the linear-growth region, ignoring non-linear interactions of disturbances. Herbert [1] suggested the parabolized stability equation (PSE) which overcomes the LST limitation. PSE is successfully validated in the overall transition region including the final stage of the transition [2,3]. Since the computational cost of PSE computations grow exponentially as high-order nonlinear

interactions initiate, it is not efficient to continuously use PSE in the turbulent region where the nonlinear interaction occurs in a broad range of the turbulence spectrum.

Direct-numerical simulation (DNS) can be used for the all range of the turbulent transition in a boundary layer, resolving all the relevant scales and their nonlinear interactions, and subsequent turbulent boundary layer [4,5,6]. It is, however, not efficient to use DNS in a practical situation because of the high computational cost.

In this study, we pursue an LES framework where PSE is incorporated for disturbances in the pre-transitional region. According to the study of Jee et al. [7], LES combined with LST is able to reduce the computational cost, and accurately resolve nonlinear interactions. In contrast to the previous study [7], PSE is coupled with LES here.

To demonstrate the feasibility of LES coupled with PSE, a canonical case is chosen: transition in a zero-pressure gradient on a flat plate. Kachanov and Levchenko conducted experiments with a vibrating ribbon, assigning two-dimensional (2D) Tollmien-Schlichting (TS) wave and sub-harmonic three-dimensional (3D) oblique waves [8]. Following the experimental conditions, 2D TS and 3D oblique waves are computed using PSE.

2 Methodology

The current framework of LES coupled with PSE is shown in Figure 1. Laminar flow is computed first on a 2D domain including the upstream and the main LES region. Disturbance modes, obtained from PSE, are superimposed to the laminar solution at $\sqrt{Re_x} = 400$ which is the inlet of the LES computation. Each plane figure in Figure 1 indicates each velocity component, which consists of the superimposed disturbances and the laminar solution. Nonlinear interactions between disturbances and the subsequent turbulent transition are the expected to be captured in the current LES computation.

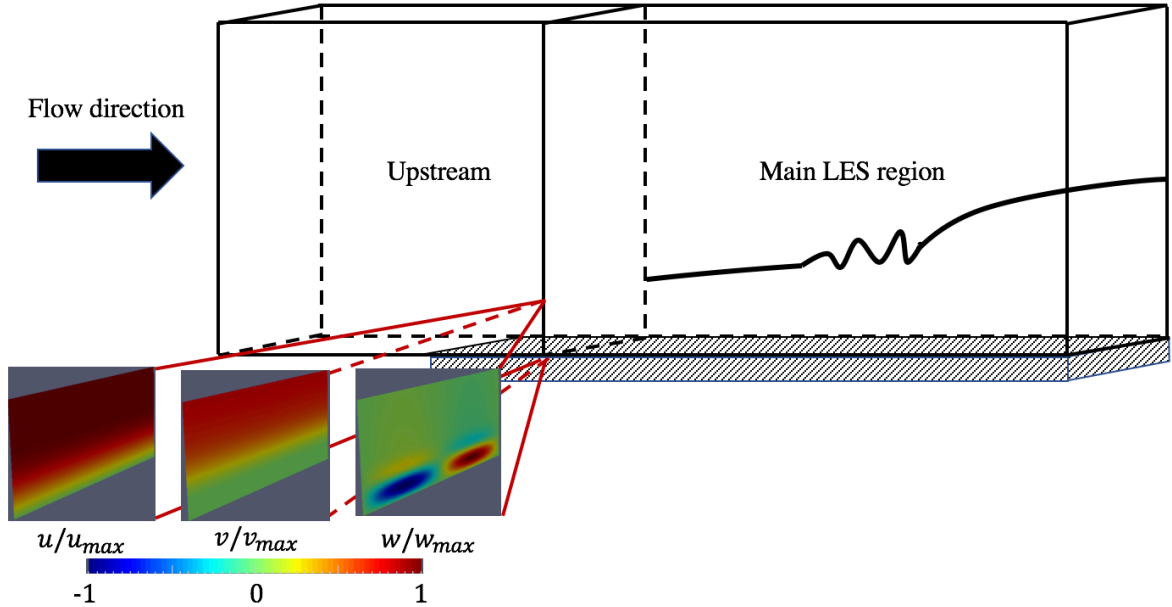


Figure 1: Schematic diagram of the current LES framework.

2.1 The Stability Analysis

A disturbance u' can be expressed as the following Equation (1).

$$u'_i(x_i, t) = A \hat{u}_i(y) \exp [i(\alpha x + \beta z - \omega t)] \quad (1)$$

Where A is the disturbance maximum amplitude, $\hat{u}_i(y)$ is the complex eigenfunction, α is the streamwise wave number, β is the spanwise wavenumber, and ω is the angular frequency. The quasi-parallel assumption is used in Equation (1). The oblique angle is determined with the two wave numbers $\theta = \arctan(\beta/\alpha)$. The streamwise wave length is $\lambda_x = 2\pi/\alpha$, whereas the spanwise wave length $\lambda_z = 2\pi/\beta$.

A 2D TS and 3D oblique waves are obtained from the stability analysis using PSE. Disturbance mode shapes at inlet $\sqrt{Re_x} = 400$ are shown in Figure 2. Current mode shapes are agreed well with the linear stability analysis of Jee et al. [7]. The maximum amplitude of both the TS and oblique waves appears in the streamwise disturbance u' .

The oblique wave on the inlet y - z plane are shown in Figure 3 at four selected phases. The oblique angles are $\theta = \pm 63.6^\circ$, following the experiment. Two oblique waves propagate in the opposite direction in the span, which results in the peak-valley contour.

The maximum amplitude of the 2D wave is set to be 0.46% of the freestream velocity, and maximum amplitude of the oblique wave is 0.01%, following the PSE condition of Esfahanian et al. [3].

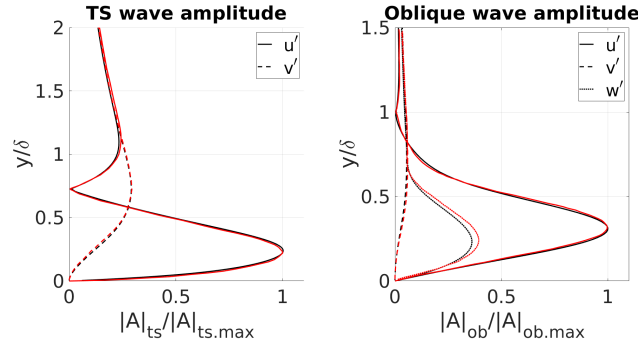


Figure 2: Amplitudes of the TS wave and the oblique wave. Black lines: current PSE analysis; red lines: linear stability analysis of Jee et al. [7].

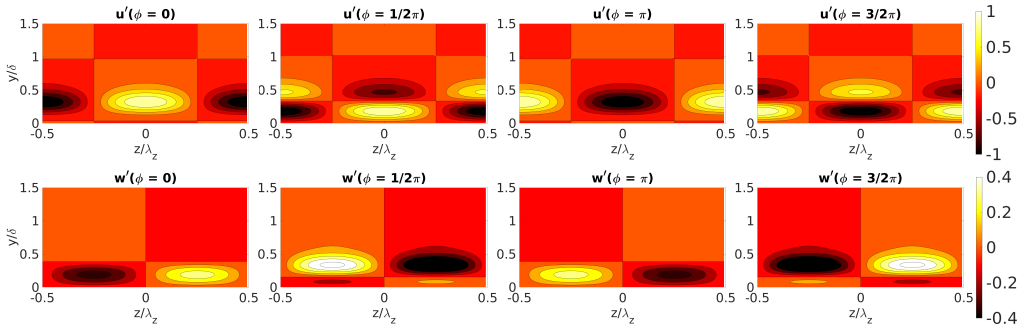


Figure 3: Oblique waves normalized by sub-harmonic's u'_{max} .

2.2 Large-Eddy Simulation

The filtered, incompressible Navier-Stokes equations (Equations 2 and 3) [9] are numerically solved with the wall-adapting local eddy-viscosity (WALE) model.

$$\frac{\partial \bar{u}_i}{\partial x_i} = 0 \quad (2)$$

$$\frac{\partial \bar{u}_j}{\partial t} + \frac{\partial}{\partial x_i} (\bar{u}_i \bar{u}_j) = \nu \frac{\partial^2 \bar{u}_j}{\partial x_i \partial x_i} - \frac{\partial \tau_{ij}^r}{\partial x_i} - \frac{1}{\rho} \frac{\partial \bar{p}}{\partial x_j} \quad (3)$$

Where the overbar indicates the filtering operation. The implicit filtering with the given grid is used in this study. The stress tensor τ_{ij}^r is modeled as follow,

$$\tau_{ij}^r = -2\nu_t \bar{S}_{ij}. \quad (4)$$

To obtain the eddy-viscosity ν_t , the WALE model (Equation 4) [10] is used, following the reference [7].

$$\nu_t = (C_w \Delta)^2 \frac{(S_{ij}^d S_{ij}^d)^{3/2}}{(\bar{S}_{ij} \bar{S}_{ij})^{5/2} + (S_{ij}^d S_{ij}^d)^{5/4}} \quad (5)$$

$$S_{ij}^d = \frac{1}{2} \left(\frac{\partial \bar{u}_i}{\partial x_k} \frac{\partial \bar{u}_k}{\partial x_j} + \frac{\partial \bar{u}_j}{\partial x_k} \frac{\partial \bar{u}_k}{\partial x_i} \right) - \frac{1}{3} \delta_{ij} \frac{\partial \bar{u}_k}{\partial x_k} \frac{\partial \bar{u}_k}{\partial x_k} \quad (6)$$

$$\bar{S}_{ij} = \frac{1}{2} \left(\frac{\partial \bar{u}_i}{\partial j} + \frac{\partial \bar{u}_j}{\partial x_i} \right) \quad (7)$$

Since the WALE model provides essentially zero eddy viscosity for 2D flow, it is expected to be dormant in the upstream laminar region.

The 2nd-order Crank-Nicolson is used for the time integration, and the 2nd-order central difference is used for the spatial integration. The pressure-implicit with splitting of operators (PISO) algorithm is used to solve the Navier-Stokes equations. The incompressible solver OpenFOAM v4.1 is used.

The modified unsteady boundary condition is implemented the flow solver. It is required to superimpose disturbance modes to the laminar boundary solution at the inlet in the current LES. To achieve the unsteady inlet condition, the solver is modified such that the unsteady disturbances are properly fed into the LES inlet. The periodic boundary condition is applied to the spanwise direction. The pressure outlet boundary condition is used to the outlet condition and the upper boundary.

Two grid resolutions are numerically tested in this study, as listed in Table 1. The wall unit is calculated, based on the maximum value of the skin friction in the simulation. It is required to resolve disturbance modes in the laminar boundary layer. Thus, it is anticipated that the requirement of $\lambda_{TS,x}/\Delta_x \gtrsim 32$, and $\lambda_z/\Delta_z \gtrsim 32$ provide sufficiently small grids for disturbance modes, their nonlinear interactions, and subsequent turbulent boundary layer. The current time step size is $\Delta_t = T_{TS}/256$ where T_{TS} is the period of the 2D TS wave.

Table 1: Grid resolutions of current LES.

Grid	Grid points	Δx^+	Δy^+	Δz^+
Fine grid	3088×256×64	14 ($\lambda_{TS,x}/64$)	1.3	15 ($\lambda_z/64$)
Medium grid	1544×128×32	28($\lambda_{TS,x}/32$)	1.3	30 ($\lambda_z/32$)

3 Results

Turbulent transition in the boundary layer over the flat plate is reproduced in the current simulation. Instantaneous vortical structures are shown in Figure 4, using the Q criteria colored by the streamwise

velocity. For clear visualization, the domain is replicated in the spanwise direction. At the initial stage, the 2D TS wave is dominant so spanwise vortical structures are mainly visualized until the downstream location of $\sqrt{Re_x} = 650$. Undulations in the spanwise direction appear after $\sqrt{Re_x} = 650$ through enough growth of oblique waves. As 3D vortical structures become clear, staggered Λ -structures are predicted in transition regions $\sqrt{Re_x} = 650 \sim 720$. Staggered Λ -structures are associated with the H-type natural transition. After Λ -structures breakdown near $\sqrt{Re_x} = 750$, small eddies emerge. Hairpin vortical structures are also well captured in the turbulent boundary layer.

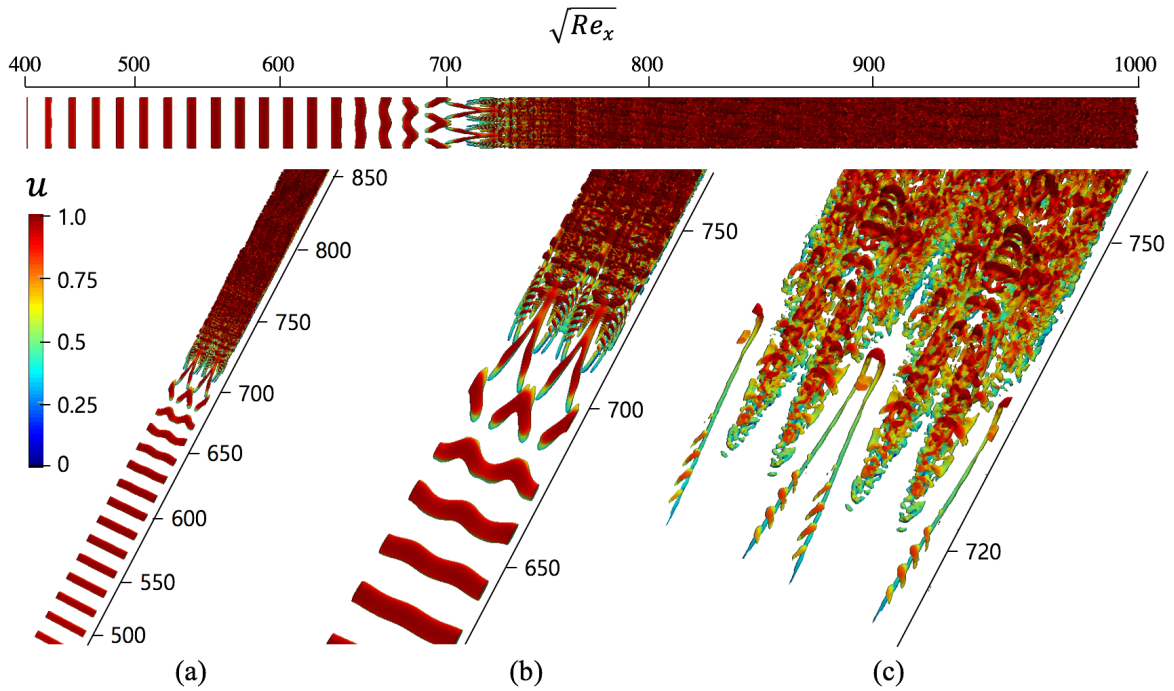


Figure 4: Instantaneous vortical structures visualized by iso volume of positive Q -criterion colored with normalized streamwise velocity. $Q > 0$ for (a) and (b); $Q > 350$ for (c).

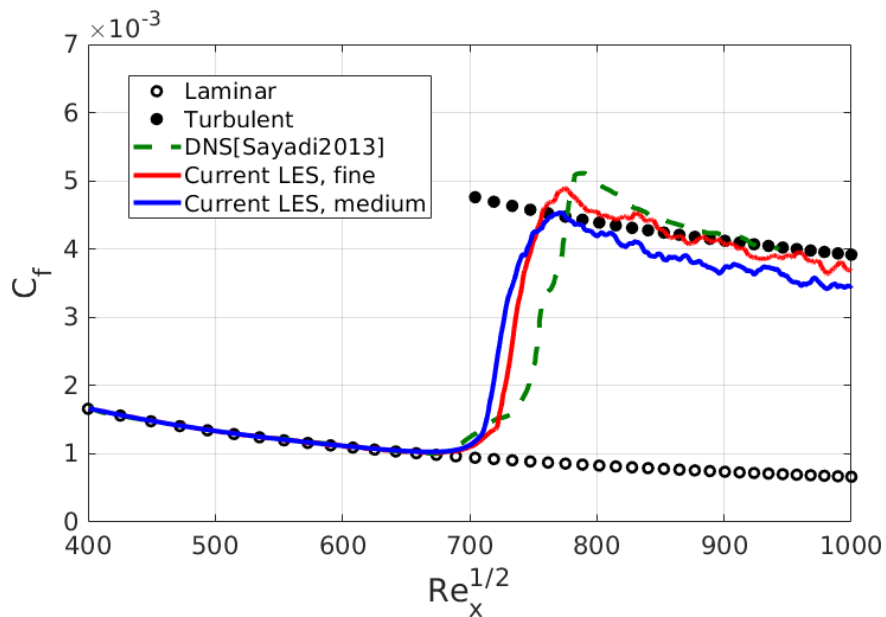


Figure 5: The skin friction along the flat plate

The skin friction is compared with the DNS study of Sayadi et al. [6] in Figure 5 along with the Blasius solution and the empirical turbulent skin friction. The deviation of the skin friction from the laminar solution is well reproduced in the current LES. The turbulent skin friction is also well reproduced in this study with the fine grid. The medium grid provides the accurate deviation from the laminar skin friction with a minor difference in the transition length, compared to the fine-grid LES. The turbulent skin friction is slightly under-estimated in the medium-grid LES.

Amplitude growths are compared with PSE results which were validated with Kachanov and Levchenko experiment in reference [2]. Figure 6 shows the maximum amplitude growth of selected instabilities modes. The 2D TS wave is denoted by $F_{2,0}$, and the sub harmonic oblique wave $F_{1,1}$, the second harmonic mode $F_{4,0}$, and third harmonic oblique mode $F_{3,1}$. Current results are well matched with the PSE analysis. After $\sqrt{Re_x} = 500$, oblique waves, $F_{1,1}$ and $F_{3,1}$, exponentially elevate whereas 2D waves, $F_{2,0}$ and $F_{4,0}$, still gradually grow. $F_{1,1}$ is larger than $F_{2,0}$ at $\sqrt{Re_x} = 650$ where vortical structures become clearly visible in the spanwise direction (see Figure 4). All modes exponentially grow from $\sqrt{Re_x} = 650$, and then the flow becomes turbulent.

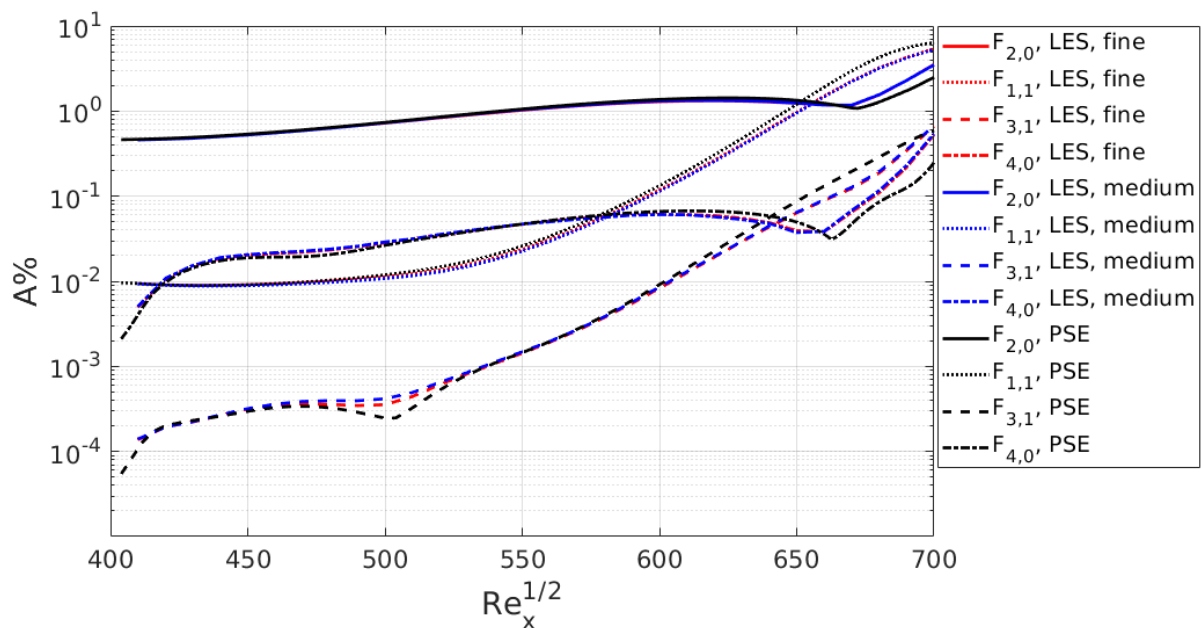


Figure 6: Maximum amplitude growth of selected instabilities modes in current computations.

The number of grid points are compared with the previous DNS [6] in Figure 7. The current LES approach coupled with PSE is able to reduce the computational cost, compared to the previous DNS. Note that a higher order numerical scheme is used in the DNS whereas the second order scheme is used in the current LES. If the proposed LES approach is used with a higher-order scheme, then the reduction in the grid count can be achieved more. In addition, it is anticipated that the computational cost can be reduced further more by moving the inlet location close to the final stage of the transition.

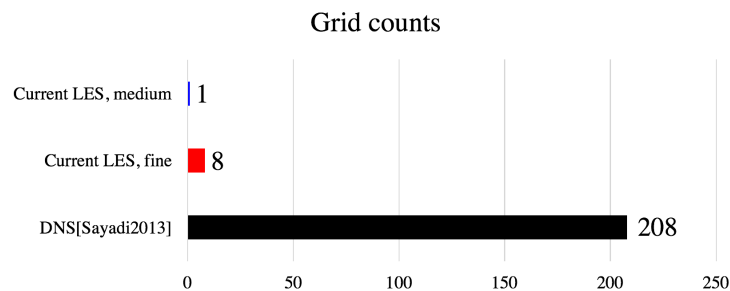


Figure 7: Comparison of grid counts in the current computations and the DNS of [6].

4 Conclusion and Future Work

Turbulent transition in the wall-bounded flow was numerically studied. In this study, LES coupled with PSE was used for efficient and accurate computations. Boundary layer disturbances were determined by PSE. The Blasius solution and disturbances were applied as the forcing condition at the LES inlet. Staggered Λ -shaped vortical structures and hairpin vortices are well reproduced in the current simulation. Current LES reproduced the transition region observed in the DNS [6]. The growth of the instabilities is also well captured, compared with PSE. Grid counts were compared with the DNS [6], and the computational cost is reduced successfully as expected.

Two main aspects are planned for future works. First, the PSE-coupled LES method can be expanded to supersonic flow. Second, the domain reduction will be studied by moving the inlet location to downstream near the final stage of the transition. It is expected that the more efficient computation will be possible with a smaller LES domain.

5 Acknowledgements

This work is carried out as part of Space Core Technology Development Program. This work was supported by the National Research Foundation of Korea(NRF) grant funded by the Ministry of Science and ICT(MSIT) of Korea government. (NRF-2017M1A3A3A02016810). This work is also supported by the National Institute of Supercomputing and Network/Korea Institute of Science and Technology Information with supercomputing resources including technical support (Project No. KSC-2017-C3-0048).

References

- [1] T. Herbert. Parabolized stability equations. *Ann. Rev. of Fluid Mech.*, 29(1):245-283, 1997.
- [2] D. Park and S. O. Park. Linear and non-linear stability analysis of incompressible boundary layer over a two-dimensional hump. *Computers & Fluids*, 73:80-96, 2013.
- [3] V. Esfahanian, K. Hejranfar, and F. Sabetghadam. Linear and nonlinear PSE for stability analysis of the Blasius boundary layer using compact scheme. *J. of Fluids Eng.*, 123(3):545-550, 2001.
- [4] R. D. Joslin, C. L. streett, and C. L. Chang. Spatial direct numerical simulation of boundary-layer transition mechanism: validation of PSE theory. *Theor. Comput. Fluid Dyn.*, 4:271-288, 1993.
- [5] H. F. Fasel, U. Rist, and U. Konzelmann. Numerical investigation of the three-dimensional development in boundary-layer transition. *AIAA journal*, 28(1):29-37, 1990.
- [6] T. Sayadi, C. W. Hamman, and P. Moin, Direct numerical simulation of complete H-type and K-type transitions with implications for the dynamics of turbulent boundary layers. *J. Fluid Mechanics*, 724:480-509, 2013.
- [7] S. Jee, J. Joo, and R. Lin. Transitional flow computations using Large-eddy simulation combined with the boundary layer stability theory. *Asia-Pacific International Symposium on Aerospace Technology*, Seoul, Korea, 2017.
- [8] Y.S. Kachanov and V.Y. Levchenko. The resonant interaction of disturbances at laminar-turbulent transition in a boundary layer. *J. Fluid Mechanics*, 138:209-247, 1984.
- [9] S. B. Pope. *Turbulent Flows*. Cambridge University Press, 558-639, 2001
- [10] F. Nicoud and F. Ducros. Subgrid-scale stress modelling based on the square of the velocity gradient tensor. *Flow, turbulence and Combustion*, 62(3):183-200, 1999.